PHYSICAL REVIEW E **71**, 061706 (2005)

Waves at the nematic-isotropic interface: Thermotropic nematogen–non-nematogen mixtures

V. Popa-Nita
Faculty of Physics, University of Bucharest, P.O. Box MG-11, Bucharest 76900, Romania

T. J. Sluckin
School of Mathematics, University of Southampton, Southampton SO17 1BJ, United Kingdom

S. Kralj
Laboratory of Physics of Complex Systems, Faculty of Education, University of Maribor, Koroška 160, 2000 Maribor, Slovenia

(Received 17 December 2004; published 20 June 2005)

We develop a theory for surface modes at the nematic-isotropic interface in thermotropic nematogen–non-nematogen mixtures. We employ the dynamical generalization of the Landau–de Gennes model for the orientational (nonconserved) order parameter, coupled with the Cahn-Hilliard equation for concentration (conserved parameter), and include hydrodynamic degrees of freedom. The theory uses a generalized form of the Landau–de Gennes free-energy density to include the coupling between the concentration of the non-nematogen fluid and the orientational order parameter. Two representative phase diagrams are shown. The method of matched asymptotic expansions is used to obtain a generalized dispersion relation. Further analysis is made in particular cases. Orientational order parameter relaxation dominates in the short-wavelength limit, while in the long-wavelength limit viscous damping processes become important. There is an intermediate region (depending on the temperature) in which the interaction between conserved parameter dynamics and hydrodynamics is important.

DOI: 10.1103/PhysRevE.71.061706 PACS number(s): 61.30.Cz, 64.70.Md, 83.80.Xz

I. INTRODUCTION

Most liquid crystals used in technological applications, such as electro-optical devices [1], are mixtures. Often we have to consider inhomogeneous mixtures between thermotropic nematogen and a non-nematogen. The dynamics of such materials involves treating not only the orientational order but also the concentration of nematogen. However, in a dynamical theory these two—coupled—variables have a different status. Orientational order is a *nonconserved* order parameter and normally relaxes diffusively. By contrast, concentration is a *conserved* order parameter, and relaxes through an induced current. The coupling of a conserved order parameter to a nonconserved order parameter, even when the latter is in some sense the driving force in the system, thus has profound effects on the dynamics. A subset of these effects is the subject of this paper.

In these systems, a biphasic region between the isotropic and the nematic phases appears below the nematic-isotropic transition temperature of the pure nematogen. When the system is thermally quenched from the stable isotropic phase into the biphasic region, fluctuations of concentration and of orientational order occur, and isotropic or nematic droplets can appear. By whatever early stage process, e.g. nucleation or spinodal decomposition, domain walls—otherwise known as interfaces—soon form.

In this paper, we analyze the problem of damping of capillary waves at these interfaces. In the case of a pure nematogen compound, very different dispersion relations for waves at the nematic-isotropic interface can be derived depending on the way the calculations are done. More precisely, the diffuse interface model, solved by assuming that the order parameter and velocity fields do not interact, leads to purely diffusive surface waves whose mode structure is identical to that of the bulk diffusive modes found in the time-dependent Ginzburg-Landau equation [2]. However, for the same problem, the sharp interface model yields modified capillary waves, with a large propagating component.

In the two previous papers [3,4], we have examined this problem for a simpler system in which there was only one component. The two points of view have been reconciled by analyzing the surface eigenmodes of the nematic-isotropic interface within the Hess-Olmsted-Goldbart-Qian-Sheng phenomenological model [5–7] of nematogenic fluids. In [3], it was assumed that the nematic director is fixed in space and time, so that the relevant physics was only described by a scalar order parameter. It turns out that this assumption is only valid if the interfacial tension is isotropic. This required that (a) the surface tension does not depend on the director orientation at the interface, and (b) (less obviously) *backflow*, i.e., coupling between the flow and the director, can be neglected. A general dispersion relation was then obtained, having as particular cases two different regimes. In the short-wavelength limit, the interface is diffusive and the relaxation of the order parameter is the dominant process. By contrast, in the long-wavelength limit, the interface is sharp and the viscous damping process dominates. For pentylcyanobiphenyl (5CB), the transition between these two regimes takes place at $\lambda_c = 5\ \mu$m, which should be visible experimentally.

In [4], we reconsidered the problem in a more general way, taking into account both the hydrodynamic coupling with the director and the surface tension anisotropy, which can be as large as 20% at the nematic-isotropic interface. As a result, interface oscillations couple with the director field via hydrodynamic flow and backflow effects. In the general dispersion relation, three distinct regions can be distinguished: (i) at very large values of λ ($\lambda > \lambda_{c_1} \simeq 6$ cm), the dissipation due to shear flow dominates and the nematic behaves as a viscous isotropic fluid; (ii) at intermediate values of λ ($\lambda_{c_2} \simeq 1 \times 10^{-4}$ cm $< \lambda < \lambda_{c_1}$), curvature elasticity and backflow effects become important; and finally (iii) at low values of λ ($\lambda < \lambda_{c_2}$), the relaxation of the order parameter governs the physics. The numerical values λ_{c_1} and λ_{c_2} correspond to 5CB. The influence of the anisotropy of the surface tension and of the hydrodynamic coupling between the flow and the director has a fairly small effect ($\simeq -20\%$) on the relaxation rate. By contrast, the influence on the phase velocity is very important in the second region, in which a new propagating mode is observed. The effect of the rotational viscosity and the associated backflow effect are much more important than that of the anchoring energy.

In this paper, we extend this analysis to the nematic-isotropic interface in thermotropic nematogen–non-nematogen mixtures. The new physics involves coupling time-dependent Ginzburg-Landau and Cahn-Hilliard equations [8] with hydrodynamic degrees of freedom. A similar model has been used to study the nematic-isotropic interface in a polymer-nematic mixture [9] and the behavior of a suspension of rigid rod particles in shear flow [10] in the framework of the Doi model [11].

The unperturbed or base state of the system is a planar nematic-isotropic interface in equilibrium. This condition fixes its temperature. To simplify, we further assume that the temperature is uniform. There is thus no temperature gradient perpendicular to the interface. Due to thermal fluctuations, small amplitude monochromatic waves develop at the interface. We use a linear stability analysis of the equations to obtain their dispersion relation.

The paper is organized as follows. In the next section, we introduce the free energy of a nonuniform thermotropic nematogen–non-nematogen mixture system. We present the static phase diagrams and derive the interfacial tension between coexisting phases. In Sec. III, we give the governing equations. We then present in Sec. IV the dispersion relations corresponding to the two regions defined by the typical lengths in the problem. The general dispersion relation and numerical results are presented in Sec. V. In Sec. VI, we draw some conclusions and present directions for future work.

II. FREE ENERGY

A thermotropic nematic–non-nematic mixture is characterized by a conserved parameter and a nonconserved parameter. The conserved parameter is the concentration $c = N_1/N$ of the non-nematic component, where N_1 is the number of molecules of non-nematic component and N the total number of molecules. The nonconserved parameter is the orientational nematic order parameter $Q_{\alpha\beta}$. The orientational order parameter is a traceless symmetric second rank tensor with components given by [12,13]

$$Q_{\alpha\beta} = S(3n_\alpha n_\beta - \delta_{\alpha\beta})/2, \tag{1}$$

where the unit vector $\vec{n}$ is the nematic director and S is the usual scalar order parameter. $S=0$ in the isotropic liquid and $S=1$ in a fully oriented nematic phase. In this paper, we shall simplify by supposing $\vec{n}$ to be fixed in space and time, and the relevant physics is given by the scalar order parameter $S(\vec{r},t)$. We note that this is an idealization which is in general not true during the relaxation, and even not true close to the interface. However, previous studies [2] suggest that the slowest relaxation modes approximately fulfill this condition when the director anchoring is homeotropic at the interface. In a later work, we shall relax this approximation.

Within the mesoscopic approach, the free-energy functional is given by

$$F[c,Q_{\alpha\beta}] = \int \left[f(c,Q_{\alpha\beta}) + \frac{1}{2}K_c(\vec{\nabla}c)^2 + K_0(\partial_\alpha c)(\partial_\beta Q_{\alpha\beta}) + \frac{1}{2}L_1(\partial_\gamma Q_{\alpha\beta})^2 + \frac{1}{2}L_2(\partial_\alpha Q_{\alpha\beta})^2 \right] dV, \tag{2}$$

where K_c and K_0 are phenomenological coefficients. The elastic constants L_1 and L_2 are related to the Frank-Oseen elastic constants by the relations $K_1 = K_3 = 9S_n^2(L_1 + L_2/2)/2$ and $K_2 = 9S_n^2 L_1/2$, where S_n is the bulk nematic order parameter. In the so-called "one-constant approximation" ($K_1 = K_2 = K_3 = 9K_S/2$) and $S_n = 1$, $L_1 = K_S$ and $L_2 = 0$, values which we consider in this paper. The bulk free-energy density $f(c,Q_{\alpha\beta})$ consists of two parts,

$$f(c,Q_{\alpha\beta}) = f_{\mathrm{mix}}(c) + f_{\mathrm{nem}}(c,Q_{\alpha\beta}). \tag{3}$$

The first term is the free-energy density of the isotropic mixing for the two components, which governs phase separation. According to the Flory theory, the free-energy density is given by [14]

$$f_{\mathrm{mix}}(c) = \frac{Nk_BT}{V}[(1-c)\ln(1-c) + c\ln c + \chi c(1-c)], \tag{4}$$

where k_B is the Boltzmann constant, T is the absolute temperature, and $\chi = (U_0/k_BT)$ is the Flory-Huggins interaction parameter related to isotropic interaction between unlike molecular species [14].

The second term in Eq. (3) is the Landau–de Gennes free-energy density, which governs the isotropic-nematic phase transition,

$$f_{\mathrm{nem}}(c,Q_{\alpha\beta}) = (1-c)\{a[T-(1-c)T^*]Q_{\alpha\beta}Q_{\beta\alpha} - BQ_{\alpha\beta}Q_{\beta\gamma}Q_{\gamma\alpha} + C(Q_{\alpha\beta}Q_{\beta\alpha})^2\}. \tag{5}$$

The coupling between c and $Q_{\alpha\beta}$ in Eq. (5) results from microscopic considerations. According to Humphries-James-Luckhurst theory on a binary mixture [15], the orientational free energy per molecule in a mean-field approximation is given by

$$f/Nk_BT = -\frac{(1-c)^2uS^2}{2} + (1-c)\int f(\beta)\ln f(\beta)\sin\beta d\beta, \tag{6}$$

where the strength of the molecular field is determined by the molecular anisotropy u, β is the angle between the symmetry axis of the (cylindrically symmetric) molecule and the director, and $f(\beta)$ is the singlet orientational distribution function. The first term is the internal energy per molecule, while the second one represents the decrease of entropy due to the nematic ordering. The free energy given in Eq. (6) can be compared with the Landau–de Gennes expansion [16]. The consequence is that only the T^* term in Landau–de Gennes free energy comes from the internal energy, while the other terms result from the entropy expansion.

For a pure nematogen, using the form (1) for $Q_{\alpha\beta}$, the bulk free-energy density has the well-known form

$$f(S) = \frac{3}{2}a(T-T^*)S^2 - \frac{3}{4}BS^3 + \frac{9}{4}CS^4, \tag{7}$$

which describes a first-order nematic-isotropic phase transition. For $T=T_{\mathrm{NI}}=T^*+B^2/24aC$, the two phases—nematic ($S_{\mathrm{nem}}=B/6C$) and isotropic ($S_{\mathrm{iso}}=0$)—coexist in equilibrium. T^* is the undercooling limit temperature of the isotropic phase.

A. Phase diagrams

The calculation of static phase diagrams requires only the bulk free-energy density. We now nondimensionalize the free energy. The orientational order parameter is normalized with respect to its value at the transition $\overline{S}=S/S_{\mathrm{nem}}$, using the reduced temperature $\tau=(T-T^*)/(T_{\mathrm{NI}}-T^*)$. The dimensionless free-energy density is now $\overline{f}=f/f_0$, where $f_0=B^4/24^2C^3$. Omitting the bar notation, the nondimensional free-energy density becomes

$$\begin{aligned} f(c,S) = {} & \Gamma[(1-c)\ln(1-c) + c\ln c + \chi c(1-c)] \\ & + (1-c)[(\tau+\lambda c)S^2 - 2S^3 + S^4], \end{aligned} \tag{8}$$

where $\Gamma=Nk_BT/Vf_0$ and $\lambda=24aCT^*/B^2$. Now, for a pure nematogen the phase-transition temperature is $\tau_{\mathrm{NI}}=1$ and the corresponding value of the nematic orientational order parameter is $S_{\mathrm{nem}}=1$.

The equilibrium conditions can be written as [17]

$$\Delta g(c,S) = 0, \quad \frac{\partial \Delta g}{\partial c}(c,S) = 0, \quad \frac{\partial \Delta g}{\partial S}(c,S) = 0, \tag{9}$$

where $\Delta g(c,S)=f(c,S)-f(c_{\mathrm{iso}},0)-\mu(c-c_{\mathrm{iso}})$ is the difference in Gibbs free-energy density between the two phases and $\mu=(\partial f/\partial c)(c_{\mathrm{iso}},0)$ is the chemical potential.

We now introduce two representative phase diagrams for nematic–non-nematic mixture, plotted on the temperature-concentration plane. The coexistence curves (binodals) in these phase diagrams were calculated numerically, by finding pairs of states with equal chemical potentials and pressures. This is equivalent to minimization of Δg with respect to the nonconserved order parameter S [the third equation in Eqs. (9)], followed by a common tangent to a pair of points on the curve $f(c)$ [17] [the first two equations in Eqs. (9)]. The spinodal line, which separates metastable from unstable compositions, is given by the inflection point of the Gibbs free-energy density ($\partial^2\Delta g/\partial c^2=0$).

The corresponding phase diagrams are plotted in Fig. 1. The solid curves refer to the binodal and the dotted lines shows the hidden first-order nematic-isotropic transition, where the isotropic and nematic branches of the Gibbs free-energy density are equal. The dashed-dotted lines are the spinodals. Figure 1(a) shows the phase diagram for $\Gamma=\lambda=\chi=1$. For this value of the Flory-Huggins interaction parameter, the free-energy density $f(c,0)$ Eq. (8) does not predict a spinodal decomposition in the isotropic region (thus there is only one isotropic phase in the phase diagram). For temperatures below T_{NI} ($\tau_{\mathrm{NI}}=1$), there exists a two-phase coexistence region between an isotropic and a nematic phase (I+N). On decreasing the temperature (note that the undercooling limit temperature for isotropic phase T^* in the pure nematogen corresponds to $\tau^*=0$), the biphasic region broadens. Within the biphasic region, there are two different metastable regions: an isotropic metastable (Im) and a nematic metastable (Nm) region, as well as an unstable region of the nematic (Nu).

For a higher value of the Flory-Huggins interaction parameter, the phase diagram develops a triple point. Figure 1(b) shows the phase diagram for $\Gamma=\lambda=1$ and $\chi=2.5$. For

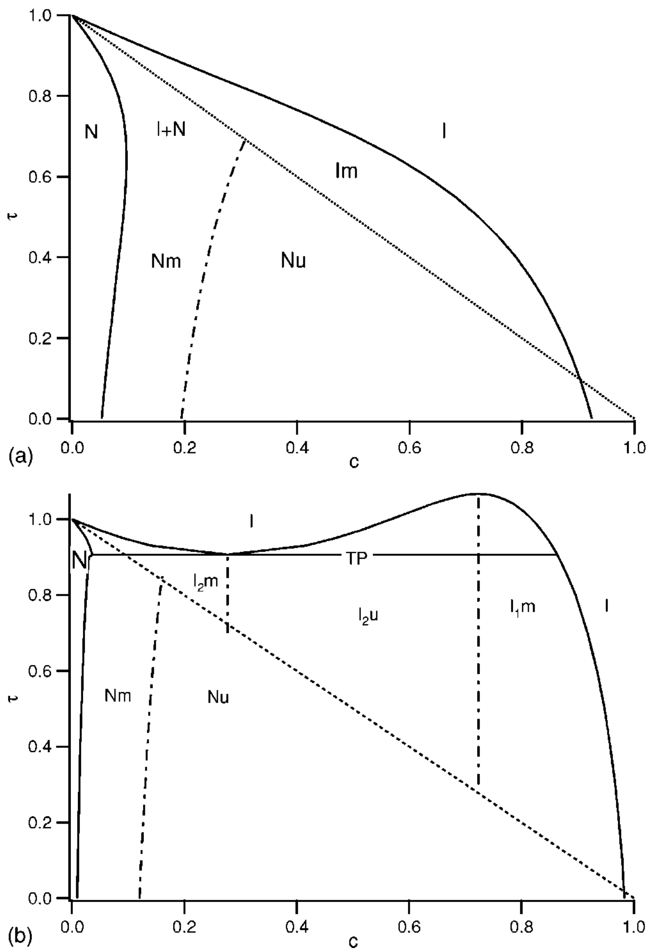

FIG. 1. Phase diagram for nematic–non-nematic binary mixture. The solid curve refers to the binodal, the dotted line shows the hidden nematic-isotropic phase transition, and the dashed-dotted line is the spinodal. (a) $\Gamma=\lambda=1$ and $\chi=1$. Below $\tau=\tau_{\mathrm{NI}}=1$, a region of two-phase coexistence exists between isotropic and nematic phases ($I+N$). (b) $\chi=2.5$ and the other parameters are the same as in (a). At $\tau=0.906$ there is a triple point (TP) where two isotropic phases (I_1+I_2) and a nematic phase (N) can simultaneously coexist.

this value of χ, there is a (classical) phase separation even in the isotropic region (thus there are two isotropic phases I_1 and I_2); I_1 (I_2) refers to the isotropic liquid phase of higher (lower) concentration on the phase diagram. The arrow shows the critical point for the I_1+I_2 phase separation. At $\tau=0.906$, there is a triple point (TP) where the two isotropic phases and the nematic phase can simultaneously coexist. There are two spinodal (unstable) regions in the phase diagram, i.e., an isotropic spinodal region (I_2u) and a nematic spinodal region (Nu), which are separated by the hidden nematic-isotropic transition line. Similar phase diagrams have been obtained by other workers for polymeric–liquid-crystals mixture [18].

In both phase diagrams, we can distinguish two different regions. Near $\tau=1$, the concentration jump at the transition is very small, so that the important effect results from the nonconserved order parameter variation. On decreasing temperature, the concentration jump at the transition is larger and the variation of the conserved parameter becomes important.

B. Interfacial tension

We consider a planar nematic-isotropic interface of area $\mathcal{A}$ in equilibrium in the nematic–non-nematic mixture and take the z axis perpendicular to the interface. The free-energy functional (2) can be expressed as

$$F[c,S] = \mathcal{A}\int_{-\infty}^{\infty} dz\left[f(c,S) + \frac{1}{2}K_c(\partial_z c)^2 + K_0(\partial_z c)(\partial_z S) + \frac{1}{2}K_S(\partial_z S)^2\right]. \tag{10}$$

We rewrite Eq. (10) in dimensionless form by measuring length in unit of $l_S=(K_S S_{\mathrm{nem}}^2/f_0)^{1/2}$ and introducing the dimensionless quantities $\overline{K_c}=K_c/K_S S_{\mathrm{nem}}^2$, $\overline{K_0}=K_0/K_S S_{\mathrm{nem}}$, and $\overline{F}=F/\mathcal{A}f_0 l_S$. Omitting the bar notation, Eq. (10) can be rewritten as

$$F[c,S] = \int_{-\infty}^{\infty} dz\left[f(c,S) + \frac{1}{2}K_c(\partial_z c)^2 + K_0(\partial_z c)(\partial_z S) + \frac{1}{2}(\partial_z S)^2\right]. \tag{11}$$

The interfacial tension γ is defined as the difference, per unit area of the interface, between the free energy of the system and that of the two phases if each were uniform and isolated. Hence in nondimensional form it can be written as

$$\gamma = \int_{-\infty}^{\infty} dz\left[\Delta g(c,S) + \frac{1}{2}K_c(d_z c)^2 + K_0(d_z S)(d_z c) + \frac{1}{2}(d_z S)^2\right]. \tag{12}$$

Minimizing the functional in Eq. (12) with respect to $c(z)$ and $S(z)$, we obtain the corresponding Euler-Lagrange equations for the equilibrium profiles of the order parameters,

$$K_c d_z^2 c_0 + K_0 d_z^2 S_0 = \frac{\partial \Delta g}{\partial c}, \tag{13}$$

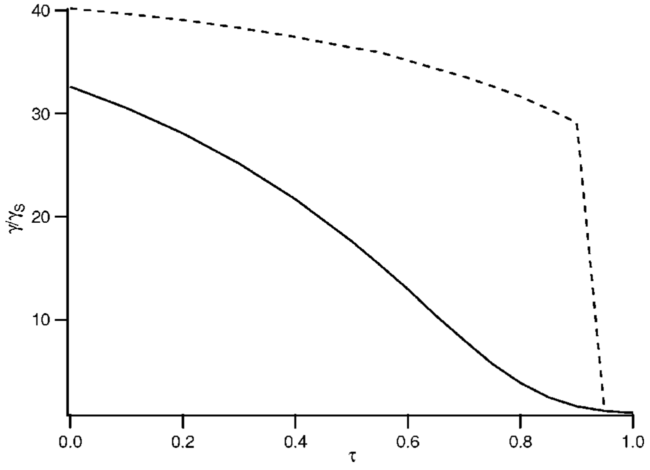

FIG. 2. Interfacial tension (γ) between the isotropic and nematic phases plotted against the reduced temperature (τ). The reduced interfacial tension γ/γ_S is normalized by the interfacial tension (γ_S) for the isotropic-nematic interface of the pure nematogen. Solid line: $\Gamma=\lambda=\chi=1$. Dashed line: $\Gamma=\lambda=1$ and $\chi=2.5$.

$$d_z^2 S_0 + K_0 d_z^2 c_0 = \frac{\partial \Delta g}{\partial S}, \tag{14}$$

with the following boundary conditions:

$$(c,S) = \begin{cases} (c_{\mathrm{nem}}, S_{\mathrm{nem}}) & \text{as } z \to -\infty, \\ (c_{\mathrm{iso}}, 0) & \text{as } z \to \infty, \end{cases} \tag{15}$$

and $d_z c(\pm\infty)=d_z S(\pm\infty)=0$.

Multiplying Eq. (13) by $d_z c$ and Eq. (14) by $d_z S$, adding the resulting equations, and then integrating once with respect to z, we obtain the condition for a planar equilibrium interface solution,

$$\Delta g = \frac{1}{2}K_c(d_z c)^2 + K_0(d_z S)(d_z c) + \frac{1}{2}(d_z S)^2. \tag{16}$$

Using this expression to eliminate the gradient terms from Eq. (12), the interfacial tension becomes

$$\gamma = 2\int_{-\infty}^{\infty} \Delta g(c(z),S(z))dz. \tag{17}$$

To perform numerical calculations, we have taken values for the bulk Landau–de Gennes free-energy parameters which correspond to 5CB: $a=3.3\times10^5$ erg/K cm^3, $B=8.9\times10^6$ erg/cm^3, and $C=5.6\times10^6$ erg/cm^3 [19], which gives $f_0=8.6\times10^3$ erg/cm^3, and the typical experimental values given in the literature: $K_S=2.1\times10^{-7}$ dyn, $K_c=K_0=8.4\times10^{-6}$ dyn, and $\gamma_S=1\times10^{-2}$ erg/cm^2 (γ_S is the nematic-isotropic interfacial tension for a pure nematogen) [13,18,20,21]. By numerically solving the Euler-Lagrange equations (13) and (14), we calculate the equilibrium profiles $c(z)$ and $S(z)$ (which are very close to the well-known hyperbolic tangent profiles) and using Eq. (17) the interfacial tension for the nematic-isotropic equilibrium interface.

In Fig. 2, we plot the interfacial tension γ between the isotropic and nematic phases, as a function of the reduced temperature τ, for both phase diagrams presented in Fig. 1.

The reduced interfacial tension γ/γ_S is normalized by the interfacial tension γ_S of an isotropic-nematic interface of the pure nematogen at $\tau=\tau_{\mathrm{NI}}=1$. In the first case (for $\chi=1$, continuous line in Fig. 2), the interfacial tension is practically constant near $\tau=1$ and then increases rapidly with decreasing temperature. For $\chi=2.5$ (dashed line), the interfacial tension has a jump at critical point $\tau=\tau_c=0.906$ because the nematic-isotropic interface changes.

III. EQUATIONS OF MOTION

We assume that the heat diffusion is sufficiently rapid in order that the system remains at thermal equilibrium. We therefore ignore the equation for energy conservation and assume an isothermal system at a specified temperature. We further assume the fluid is incompressible. Within these approximations, the equations of motion for the velocity and the nematic order parameter become [5–7]

$$\partial_\alpha v_\alpha = 0, \tag{18}$$

$$\rho\frac{dv_\alpha}{dt} = \partial_\beta(-p\,\delta_{\alpha\beta} + \sigma^d_{\alpha\beta} + \sigma^v_{\alpha\beta}) + \frac{\delta F}{\delta c}\partial_\beta c\,\delta_{\alpha\beta}, \tag{19}$$

$$0 = h_{\alpha\beta} + h^v_{\alpha\beta} - \lambda\,\delta_{\alpha\beta} - \epsilon_{\alpha\beta\gamma}\lambda_\gamma, \tag{20}$$

where ρ is the density, p is the pressure, while λ and λ_γ are the Lagrange multipliers associated to conditions $\mathrm{Tr}Q=0$ and $Q_{\alpha\beta}=Q_{\beta\alpha}$, respectively. In this expression, α, β, and γ run from 1 to 3, summation over repeated indices is implied, $\epsilon_{\alpha\beta\gamma}$ is the Levi-Civita symbol, and d/dt is the total time derivative $\partial/\partial t+\vec{v}\cdot\vec{\nabla}$. The distortion stress σ^d [which results from molecular displacement keeping the orientation fixed: $\vec{r}\rightarrow\vec{r}\,'+\vec{u}(\vec{r}),Q_{\alpha\beta}(\vec{r})\rightarrow Q'_{\alpha\beta}(\vec{r}\,')=Q_{\alpha\beta}(\vec{r})$] and the elastic molecular field h [which results directly from the virtual orientational distortion: $Q_{\alpha\beta}(\vec{r})\rightarrow Q'_{\alpha\beta}(\vec{r})$] are obtained in standard manner as

$$\sigma^d_{\alpha\beta} = -\frac{\partial F}{\partial(\partial_\alpha Q_{\gamma\rho})}\partial_\beta Q_{\gamma\rho}, \tag{21}$$

$$h_{\alpha\beta} = -\,\delta F/\delta Q_{\alpha\beta}. \tag{22}$$

The viscous stress tensor σ^v and the viscous molecular field h^v are introduced through the consideration of entropy production in a dissipative flowing nematic. They are given by a tensorial generalization of the Ericksen-Leslie theory [22,23,7],

$$\begin{aligned}\sigma^v_{\alpha\beta} = {} & \beta_1 Q_{\alpha\beta}Q_{\mu\nu}A_{\mu\nu} + \beta_4 A_{\alpha\beta} + \beta_5 Q_{\alpha\mu}A_{\mu\beta} + \beta_6 Q_{\beta\mu}A_{\mu\alpha} \\ & + \frac{1}{2}\mu_2 N_{\alpha\beta} - \mu_1 Q_{\alpha\mu}N_{\mu\beta} + \mu_1 Q_{\beta\mu}N_{\mu\alpha},\end{aligned} \tag{23}$$

$$-h^v_{\alpha\beta} = -\frac{1}{2}\mu_2 A_{\alpha\beta} + \mu_1 N_{\alpha\beta}, \tag{24}$$

where

$$N_{\alpha\beta} = \frac{dQ_{\alpha\beta}}{dt} + Q_{\alpha\mu}W_{\mu\beta} - W_{\alpha\mu}Q_{\mu\beta} \tag{25}$$

is the time rate of change of the order parameter with respect to the background fluid angular velocity, sometimes known as corotational time derivative. The quantities β_1, β_4, β_5, β_6, μ_1, and $\mu_2=\beta_6-\beta_5$ are viscous coefficients which can be expressed in terms of the Leslie coefficients (α_i) and the value of the order parameter S [7], while $A_{\alpha\beta}=\frac{1}{2}(\partial_\alpha v_\beta+\partial_\beta v)$ and $W_{\alpha\beta}=\frac{1}{2}(\partial_\alpha v_\beta-\partial_\beta v_\alpha)$ are, respectively, the symmetric and antisymmetric parts of the velocity gradient tensor.

The concentration equation of motion takes the Cahn-Hilliard form [8]

$$\frac{dc}{dt} = -\vec{\nabla}\cdot\vec{J} = \Gamma_c\vec{\nabla}^2\mu, \tag{26}$$

where the transport coefficient Γ_c is assumed to be constant and the chemical potential is given by

$$\mu = \frac{\delta F}{\delta c}. \tag{27}$$

The diffusive current is $\vec{J}=-\Gamma_c\vec{\nabla}\mu$. The complete dynamics is thus describe by Eqs. (18)–(20) and (26). The dynamical equations of motion for other complex fluids have the same theoretical structure: equations of motion for the conserved quantities and the broken-symmetry or flow-induced structural (nonconserved) order parameter (analogous to $Q_{\alpha\beta}$), and a constitutive relation for the stress as a function of composition and order parameter [17].

Let us now define the three typical lengths of the problem.

(i) The first length is related to the order parameter itself. It strongly varies across the interface over a typical distance known as the microscopic correlation length $l_S=(K_S S^2_{\mathrm{nem}}/f_0)^{1/2}$ that for 5CB has the value 5×10^{-6} cm. This length gives the typical width of the order parameter profile within the interface.

(ii) The second microscopic length is related to the concentration variation inside the interface $l_c=(K_c/f_0)^{1/2}$ that for 5CB has the value 3×10^{-5} cm.

(iii) The third (macroscopic) length is associated with the vorticity, i.e., with the flow induced by the motion of the interface. The corresponding physics is described by the generalized Navier-Stokes equation (8), which can be considered in the thin interface limit. The important physical parameters are the capillary force, associated with the interfacial tension γ, the viscous dissipation, associated with viscosity coefficient η, and the fluid inertia, governed by the mass density ρ. From these three quantities, we can construct only one length $l_\eta=\eta^2/\rho\gamma$. For 5CB, $\rho=1$ g/cm^3, $\gamma=1\times10^{-2}$ erg/cm^2, and $\eta=0.1P$, so that $l_\eta=1$ cm. This length separates the inertial from the viscous regimes; the corresponding value of the Reynolds number is unity (for details, see [4]).

In the following, we shall use $t_\eta=\eta^3/\rho\gamma^2$ as unit time, which is the typical relaxation time of a perturbation of size l_η and for 5CB has the value 10 s. In the following, the ratio $\epsilon=l_S/l_\eta=l_c/l_\eta\simeq10^{-5}$ will constitute the small parameter of the theory.

We consider a two-dimensional flow with horizontal and vertical velocity components u and w in the x and z directions, respectively, and we simplify the expressions (23) and (24) by assuming that

$$\beta_1 = \beta_5 = \beta_6 = 0, \quad \beta_4 = 2\beta, \tag{28}$$

which give $\mu_2 = 0$ [7]. In terms of Leslie coefficients α_i, these relations are equivalent to

$$\alpha_1 = \alpha_5 = \alpha_6 = 0, \quad -\alpha_2 = \alpha_3 = \alpha = 9S^2\mu_1/4, \quad \alpha_4 = \beta_4 = 2\beta. \tag{29}$$

Within these approximations, the coefficient β describes the dissipation due to shear flow (shear viscosity), while μ_1 is associated to the standard rotational viscosity $\gamma_1 = \alpha_3 - \alpha_2 = 2\alpha = 9S^2\mu_1/2$.

Using these hypotheses and Eqs. (1)–(5), the basic Eqs. (18)–(20) and (26) take the following form:

$$0 = \partial_x u + \partial_z w, \tag{30}$$

$$\rho\frac{du}{dt} = -\partial_x p + \eta\vec{\nabla}^2 u - (K_S\vec{\nabla}^2 S + K_0\vec{\nabla}^2 c)\partial_x S + \left(\frac{\partial f}{\partial c} - K_c\vec{\nabla}^2 c - K_0\vec{\nabla}^2 S\right)\partial_x c, \tag{31}$$

$$\rho\frac{dw}{dt} = -\partial_z p + \eta\vec{\nabla}^2 w - (K_S\vec{\nabla}^2 S + K_0\vec{\nabla}^2 c)\partial_z S + \left(\frac{\partial f}{\partial c} - K_c\vec{\nabla}^2 c - K_0\vec{\nabla}^2 S\right)\partial_z c, \tag{32}$$

$$\frac{3\mu_1}{2}\frac{dS}{dt} = -\frac{\partial f}{\partial S} + K_S\vec{\nabla}^2 S + K_0\vec{\nabla}^2 c, \tag{33}$$

$$\frac{dc}{dt} = \Gamma_c\vec{\nabla}^2\left(\frac{\partial f}{\partial c} - K_c\vec{\nabla}^2 c - K_0\vec{\nabla}^2 S\right), \tag{34}$$

where $\eta = (\alpha + 2\beta)/2$. This viscosity corresponds to the second Miesowicz viscosity η_b [13], i.e., to the viscosity of the nematic phase when it is sheared parallel to the director.

We rewrite Eqs. (30)–(34) in dimensionless forms by measuring length in units of l_η, and time in units of t_η. We use the same scaling as in Sec. II A for the orientational order parameter and for the free-energy density, and we introduce the dimensionless quantities

$$\overline{\rho} = \frac{l_\eta^2}{f_0 t_\eta^2}\rho, \quad \overline{p} = \frac{p}{f_0}, \quad \overline{\eta} = \frac{\eta}{t_\eta f_0},$$

$$\overline{\mu_1} = \frac{3S_{\text{nem}}^2}{2t_\eta f_0}\mu_1, \quad \overline{\Gamma_c} = \frac{t_\eta}{l_\eta^2 f_0}\Gamma_c. \tag{35}$$

Omitting the bar notation in the following, we obtain

$$0 = \partial_x u + \partial_z w, \tag{36}$$

$$\rho\frac{du}{dt} = -\partial_x p + \eta\vec{\nabla}^2 u - \epsilon^2(\vec{\nabla}^2 S + \vec{\nabla}^2 c)\partial_x S + \left(\frac{\partial f}{\partial c} - \epsilon^2\vec{\nabla}^2 c - \epsilon^2\vec{\nabla}^2 S\right)\partial_x c, \tag{37}$$

$$\rho\frac{dw}{dt} = -\partial_z p + \eta\vec{\nabla}^2 w - \epsilon^2(\vec{\nabla}^2 S + \vec{\nabla}^2 c)\partial_z S + \left(\frac{\partial f}{\partial c} - \epsilon^2\vec{\nabla}^2 c - \epsilon^2\vec{\nabla}^2 S\right)\partial_z c, \tag{38}$$

$$\mu_1\frac{dS}{dt} = -\frac{\partial f}{\partial S} + \epsilon^2\vec{\nabla}^2 S + \epsilon^2\vec{\nabla}^2 c, \tag{39}$$

$$\frac{dc}{dt} = \Gamma_c\vec{\nabla}^2\left(\frac{\partial f}{\partial c} - \epsilon^2\vec{\nabla}^2 c - \epsilon^2\vec{\nabla}^2 S\right), \tag{40}$$

where $\epsilon^2 = l_S^2/l_\eta^2 = l_c^2/l_\eta^2 = l_0^2/l_\eta^2$ with $l_0 = (K_0 S_{\text{nem}}/f_0)^{1/2}$.

In what follows, we shall suppose that the stationary planar nematic-isotropic interface (i.e., the base state of the system) is situated at $z=0$, such that the nematic lies in the region $z<0$ and the isotropic phase in the region $z>0$. The x axis is taken in the direction of the wave vector $\vec{k}$ of the perturbation along the interface. This is possible without loss of generality, as the system is isotropic in the x and y directions, i.e., neglecting the biaxiality of the nematic phase. In this way, the wave number k represents the modulus of the two-dimensional wave vector in the plane of the interface.

IV. ASYMPTOTIC ANALYSIS FOR $\epsilon \ll 1$

To obtain the dispersion relation, we use the method of matched asymptotic expansions [24]. The method consists in matching the solution obtained in *outer* regions, where z is of the order unity, to that in an *inner* regions, in which z is small. In our case, there are two outer regions B and C, of dimension l_η, in which the dominant physics is hydrodynamic: dissipation due to shear flow. These two regions are a $z \to -\infty$ deep nematic region and a $z \to +\infty$ deep isotropic region. In the inner region A of dimension $l_S \simeq l_c \simeq l_0$, both conserved and nonconserved order parameters vary rapidly.

We expand the solution in the outer regions as regular perturbation series in ϵ^2,

$$u = u^{(0)}(x,z) + \epsilon^2 u^{(2)}(x,z) + O(\epsilon^4),$$

$$w = w^{(0)}(x,z) + \epsilon^2 w^{(2)}(x,z) + O(\epsilon^4),$$

$$c = c^{(0)}(x,z) + \epsilon^2 c^{(2)}(x,z) + O(\epsilon^4),$$

$$S = S^{(0)}(x,z) + \epsilon^2 S^{(2)}(x,z) + O(\epsilon^4). \tag{41}$$

In the inner region, we set $\zeta = x/\epsilon$ and $\xi = z/\epsilon$ and write similar expansions for the variables $\hat{u}(\zeta,\xi) = u(x,z)$, $\hat{w}(\zeta,\xi) = w(x,z)$, $\hat{c}(\zeta,\xi) = c(x,z)$, and $\hat{S}(\zeta,\xi) = S(x,z)$.

A. Outer regions: B and C

Here c and S are constant in each phase. We find that, to all orders, $(c,S)=(c_{\mathrm{nem}},S_{\mathrm{nem}})$ for $z<0$ and $(c,S)=(c_{\mathrm{iso}},0)$ for $z>0$. The leading-order problem for $u^{(0)}$ and $w^{(0)}$ in the outer region of the nematic phase B $(z<0)$ is given by

$$0=\partial_x u^{(0)}+\partial_z w^{(0)}, \tag{42}$$

$$\rho\frac{du^{(0)}}{dt}=-\partial_x p^{(0)}+\eta_N\vec{\nabla}^2 u^{(0)} \tag{43}$$

$$\rho\frac{dw^{(0)}}{dt}=-\partial_z p^{(0)}+\eta_N\vec{\nabla}^2 w^{(0)}, \tag{44}$$

where $\eta_N=(\alpha+2\beta)/2$ is the shear viscosity of the nematic phase. These equations have the same form in the outer region of the isotropic phase C $(z>0)$, but with a different shear viscosity coefficient $\eta_I=\beta$. The density difference between the isotropic and the nematic phase is usually very small, so that we can consider in a good approximation that the two fluids have the same density.

Thus, the outer problem is equivalent to the Navier-Stokes equation for an interface between two fluids with the same density but with different viscosities, subject to the incompressibility condition [25,26]. The solution corresponding to the stationary planar interface is given by $u_0^{(0)}=w_0^{(0)}=0,p_0^{(0)}=\mathrm{const}$.

We now impose a small periodic sinusoidal perturbation to the interface of the form $\xi_I=\xi_k\exp(ikx-\Omega t)$, where ξ_I is the vertical displacement of the interface with respect to its equilibrium position $z=0$. In our notation, k is the wave vector (real number) and Ω is the angular frequency. The latter quantity is generally a complex number whose real part gives the relaxation time $\tau=1/\mathrm{Re}(\Omega)$ of the wave, and the imaginary part, the phase velocity $v_p=\mathrm{Im}(\Omega)/k$.

For a nematic of large depth (region B: $-\infty<z<0$), the wavelike solutions of Eqs. (42)–(44) are of the form (for details, see [4])

$$u_N^{(0)}=(ikA_Ne^{kz}-l_NC_Ne^{l_Nz})\exp(ikx-\Omega t), \tag{45}$$

$$w_N^{(0)}=(kA_Ne^{kz}+ikC_Ne^{l_Nz})\exp(ikx-\Omega t), \tag{46}$$

$$p_N^{(0)}=p_0^{(0)}+\rho\Omega A_Ne^{kz}\exp(ikx-\Omega t). \tag{47}$$

Similarly, in the isotropic phase (region C: $0<z<\infty$),

$$u_I^{(0)}=(ikA_Ie^{-kz}+l_IC_Ie^{-l_Iz})\exp(ikx-\Omega t), \tag{48}$$

$$w_I^{(0)}=(-kA_Ie^{-kz}+ikC_Ie^{-l_Iz})\exp(ikx-\Omega t), \tag{49}$$

$$p_I^{(0)}=p_0^{(0)}+\rho\Omega A_Ie^{-kz}\exp(ikx-\Omega t), \tag{50}$$

where $l_N=k(1-\rho\Omega/\eta_Nk^2)^{1/2}$ and $l_I=k(1-\rho\Omega/\eta_Ik^2)^{1/2}$.

Equations (45)–(50) correspond to the classical sharp-interface approach, where it is assumed that the thickness of the inner region is zero. In this limit, the dispersion relation is determined by the boundary conditions at the nematic-isotropic interface, which can be taken at $z=0$ due to the smallness of the amplitude of the oscillations [25,26]. These conditions are as follows (for details, see [4]):

(i), (ii), and (iii): The x and z components of the velocity and the tangential components of the stress tensor must be continuous.

(iv) The jump of the normal component of the stress tensor is given by the Laplace law,

$$\sigma_{zz}(N)-\sigma_{zz}(I)=\gamma\frac{\partial^2\xi_I}{\partial x^2}. \tag{51}$$

After substituting solutions (45)–(50) into the boundary conditions, we obtain the dispersion relation in leading order in the outer region,

$$\Omega_\eta^2=\left[1+\frac{k(l_N^2+l_I^2)-2k^3}{(l_N+l_I)(k^2-l_Nl_I)}\right]\Omega_0^2, \tag{52}$$

where $\Omega_0^2=-\gamma k^3/2\rho$ is the capillary wave dispersion relation for ideal fluids. The quantity γ is the interfacial tension. It enters here as a parameter through Laplace's law (51). In the more generalized model discussed in this paper, it can be calculated from the inner region solution.

B. Inner region A

To look for the solutions in the inner region, we rewrite Eqs. (36)–(40) in terms of inner variables $\zeta=x/\epsilon$ and $\xi=z/\epsilon$,

$$0=\partial_\zeta\hat{u}+\partial_\xi\hat{w}, \tag{53}$$

$$\begin{aligned}\tilde{\rho}\frac{d\hat{u}}{dt}=&-\partial_\zeta p+\eta\vec{\nabla}^2\hat{u}-(\vec{\nabla}^2\hat{S}+\tilde{K}_0\vec{\nabla}^2\hat{c})\partial_\zeta\hat{S}\\&+\left(\frac{\partial f}{\partial\hat{c}}-\tilde{K}_c\vec{\nabla}^2\hat{c}-\tilde{K}_0\vec{\nabla}^2\hat{S}\right)\partial_\zeta\hat{c},\end{aligned} \tag{54}$$

$$\begin{aligned}\tilde{\rho}\frac{d\hat{w}}{dt}=&-\partial_\xi p+\eta\vec{\nabla}^2\hat{w}-(\vec{\nabla}^2\hat{S}+\tilde{K}_0\vec{\nabla}^2\hat{c})\partial_\xi\hat{S}\\&+\left(\frac{\partial f}{\partial\hat{c}}-\tilde{K}_c\vec{\nabla}^2\hat{c}-\tilde{K}_0\vec{\nabla}^2\hat{S}\right)\partial_\xi\hat{c},\end{aligned} \tag{55}$$

$$\mu_1\frac{d\hat{S}}{dt}=-\frac{\partial f}{\partial\hat{S}}+\vec{\nabla}^2\hat{S}+\tilde{K}_0\vec{\nabla}^2\hat{c}, \tag{56}$$

$$\frac{d\hat{c}}{dt}=\tilde{\Gamma}_c\vec{\nabla}^2\left(\frac{\partial f}{\partial\hat{c}}-\tilde{K}_c\vec{\nabla}^2\hat{c}-\tilde{K}_0\vec{\nabla}^2\hat{S}\right), \tag{57}$$

where $\tilde{\rho}=l_S^2\rho/f_0t_\eta^2$, $\tilde{K}_c=K_c/K_SS_{\mathrm{nem}}^2$, $\tilde{K}_0=K_0/K_SS_{\mathrm{nem}}$, and $\tilde{\Gamma}_c=t_\eta\Gamma_c/l_S^2f_0$.

The first step is to ignore the interaction between the velocity and the order parameters variations. In the leading order, omitting the tilde signs, we obtain

$$\partial_\zeta p = -(\vec{\nabla}^2\hat{S}^{(0)} + K_0\vec{\nabla}^2\hat{c}^{(0)})\partial_\zeta\hat{S}^{(0)} + \left(\frac{\partial f}{\partial\hat{c}}(\hat{c}^{(0)},\hat{S}^{(0)}) - K_c\vec{\nabla}^2\hat{c}^{(0)} - K_0\vec{\nabla}^2\hat{S}^{(0)}\right)\partial_\zeta\hat{c}^{(0)}, \tag{58}$$

$$\partial_\xi p = -(\vec{\nabla}^2\hat{S}^{(0)} + K_0\vec{\nabla}^2\hat{c}^{(0)})\partial_\xi\hat{S}^{(0)} + \left(\frac{\partial f}{\partial\hat{c}}(\hat{c}^{(0)},\hat{S}^{(0)}) - K_c\vec{\nabla}^2\hat{c}^{(0)} - K_0\vec{\nabla}^2\hat{S}^{(0)}\right)\partial_\xi\hat{c}^{(0)}, \tag{59}$$

$$\mu_1\frac{\partial\hat{S}^{(0)}}{\partial t} = -\frac{\partial f}{\partial\hat{S}}(\hat{c}^{(0)},\hat{S}^{(0)}) + \vec{\nabla}^2\hat{S}^{(0)} + K_0\vec{\nabla}^2\hat{c}^{(0)}, \tag{60}$$

$$\frac{\partial\hat{c}^{(0)}}{\partial t} = \Gamma_c\vec{\nabla}^2\left(\frac{\partial f}{\partial\hat{c}}(\hat{c}^{(0)},\hat{S}^{(0)}) - K_c\vec{\nabla}^2\hat{c}^{(0)} - K_0\vec{\nabla}^2\hat{S}^{(0)}\right). \tag{61}$$

Equations (60) and (61) constitute the model C in the Hohenberg and Halperin classification on critical dynamics [27].

We consider first an equilibrium planar nematic-isotropic interface perpendicular to the ξ axis. The horizontal momentum equation (58) is satisfied identically and the remaining equations give

$$\partial_\xi p_0 = -(d_\xi^2\hat{S}_0^{(0)} + K_0 d_\xi^2\hat{c}_0^{(0)})\partial_\xi S_0^{(0)} + \left(\frac{\partial f}{\partial\hat{c}}(\hat{c}_0^{(0)},\hat{S}_0^{(0)}) - K_c d_\xi^2\hat{c}_0^{(0)} - K_0 d_\xi^2\hat{S}_0^{(0)}\right)\partial_\xi\hat{c}_0^{(0)}, \tag{62}$$

$$d_\xi^2\hat{S}_0^{(0)} + K_0 d_\xi^2\hat{c}_0^{(0)} = \frac{\partial f}{\partial\hat{S}}(\hat{c}_0^{(0)},\hat{S}_0^{(0)}), \tag{63}$$

$$K_c d_\xi^2\hat{c}_0^{(0)} + K_0 d_\xi^2\hat{S}_0^{(0)} = \frac{\partial f}{\partial\hat{c}}(\hat{c}_0^{(0)},\hat{S}_0^{(0)}) - \mu, \tag{64}$$

where the subscript 0 refers to the equilibrium interface. We have integrated the Cahn-Hilliard equation (61) twice and employed the far-field condition that c is bounded. The quantity μ is the chemical potential, i.e., the Lagrange multiplier that ensures the conservation of the non-nematic quantity.

Equation (62) allows us to calculate the pressure field, and Eqs. (63) and (64) are the Euler-Lagrange equations which minimize the free-energy density; they have been studied in Sec. II B.

It is important to note that the interfacial tension γ which appears in the outer region dispersion relation (52) as a parameter introduced by the Laplace law (51) is now calculated from the inner region profiles of the order parameters by Eq. (17). In the following, we shall use only the phase diagram plotted in Fig. 1(a) and the corresponding interfacial tension (the continuous line in Fig. 2) to obtain the dispersion relation.

To obtain the leading-order dispersion relation in the inner region in the absence of hydrodynamics degrees of freedom, we impose small periodic perturbations to the interface in the ζ direction with wave vector k,

$$\hat{c}^{(0)}(\zeta,\xi,t) = \hat{c}_0^{(0)}(\xi) + A\mathcal{C}(\xi)\exp(ik\zeta - \Omega t),$$

$$\hat{S}^{(0)}(\zeta,\xi,t) = \hat{S}_0^{(0)}(\xi) + A\mathcal{S}(\xi)\exp(ik\zeta - \Omega t), \tag{65}$$

where the amplitude A is small. Substituting these forms into Eqs. (63) and (64), and linearizing in A, gives

$$\mu_1\Omega\mathcal{S} = -\vec{\nabla}^2\mathcal{S} - K_0\vec{\nabla}^2\mathcal{C} + \frac{\partial^2(\Delta g)}{\partial\hat{S}^2}(\hat{c}_0^{(0)},\hat{S}_0^{(0)})\mathcal{S} + \frac{\partial^2(\Delta g)}{\partial\hat{c}\partial\hat{S}}(\hat{c}_0^{(0)},\hat{S}_0^{(0)})\mathcal{C}, \tag{66}$$

$$\Omega\mathcal{C} = \Gamma_c\vec{\nabla}^2\left[K_c\vec{\nabla}^2\mathcal{C} + K_0\vec{\nabla}^2\mathcal{S} - \frac{\partial^2(\Delta g)}{\partial\hat{c}^2}(\hat{c}_0^{(0)},\hat{S}_0^{(0)})\mathcal{C} - \frac{\partial^2(\Delta g)}{\partial\hat{S}\partial\hat{c}}(\hat{S}_0^{(0)},\hat{c}_0^{(0)})\mathcal{S}\right], \tag{67}$$

where $\vec{\nabla}^2 = d_\xi^2 - k^2$. For a discussion of the independent eigenvalues corresponding to Cahn-Hilliard and time-dependent Ginzburg-Landau equations, see [28,29], respectively.

Since $k=0$ corresponds to a uniform translation of the interface, we know that $\Omega_{k=0}=0$ is the eigenvalue with the eigenfunctions $d_\xi\hat{c}_0^{(0)}$ and $d_\xi\hat{S}_0^{(0)}$ [this can be easily checked by differentiating Eqs. (13) and (14) with respect to z]. Here we concentrate only on these ground-state eigenfunctions, which are the "slow modes." In fact, a difficulty does appear at $k=0$ for the conserved order parameter. Physically, the interface in a conserved system cannot move freely using the Goldstone mode as it could in the nonconserved one. Thus, at $k=0$, the system can only satisfy conservation if it "ripples" transversely to the interface. At $k\neq 0$, a perturbation local to the interface of a form like the Goldstone mode is possible, since the conservation is taken care of by the fluctuation along the interface.

Multiplying Eq. (66) by $d_\xi\hat{S}_0^{(0)}$ and Eq. (67) by $d_\xi\hat{c}_0^{(0)}$, adding the two resulting equations, and using Eq. (16) and the definition of γ given in Eq. (17), we obtain the leading-order dispersion relation in the inner region as

$$\Omega_{Sc} = \frac{\gamma k^2}{\mu_1\int_{-\infty}^{\infty}(d_\xi\hat{S}_0^{(0)})^2 d\xi + \Gamma_c^{-1}\int_{-\infty}^{\infty}d\xi\int_{-\infty}^{\infty}d\xi' G_k(\xi-\xi')(d_\xi\hat{c}_0^{(0)})(d_{\xi'}\hat{c}_0^{(0)})}, \tag{68}$$

where

$$G_k(\xi-\xi')=\int_{-\infty}^{\infty}\frac{dq}{2\pi}\frac{\exp[iq(\xi-\xi')]}{k^2+q^2}=\frac{\exp(-k|\xi-\xi'|)}{2k}\qquad(69)$$

is the Green function for the operator $k^2-d_\xi^2$. In the limit $k\rightarrow 0$, we can replace $G_k(\xi-\xi')$ by its small-argument limit $1/2k$. This yields the leading-order dispersion relation in the inner region (in unscaled units),

$$\Omega_{Sc}=\frac{\gamma k^2}{\mu_1\int_{-\infty}^{\infty}(d_\xi\hat{S}_0^{(0)})^2 d\xi+(c_{\text{iso}}-c_{\text{nem}})^2/2\Gamma_c k}.\qquad(70)$$

The pure nonconserved order parameter dispersion relation is obtained in the limit $\tau=\tau_{\text{NI}}=1$, which gives $c_{\text{iso}}=c_{\text{nem}}$ and $\gamma=\gamma_S$, where $\gamma_S=K_S\int_{-\infty}^{\infty}(d_\xi\hat{S}_0^{(0)})^2 d\xi$ is the nematic-isotropic interfacial tension for a pure nematogen, and

$$\Omega_S=\frac{K_S}{\mu_1}k^2.\qquad(71)$$

We note that there is another time-dependent Ginzburg-Landau mode corresponding to a squeezing of the interface with the corresponding eigenvalue $\Omega_{S1}=\Omega_S+3f_0/2\mu_1$ [29] separated by a gap from the ground state, which we do not consider here.

The pure conserved order parameter dispersion relation is obtained in the limit $\mu_1=0$. This limit corresponds to freezing of the rotational motion. It can be written as

$$\Omega_c=\frac{2\gamma\Gamma_c k^3}{(c_{\text{iso}}-c_{\text{nem}})^2}.\qquad(72)$$

In the small-wavelength limit (region A_2 in Fig. 3), the relaxation of the nonconserved order parameter is the important process and

$$\Omega_{Sc}(k\rightarrow\infty)=\frac{\gamma k^2}{\mu_1\int_{-\infty}^{\infty}(d_\xi\hat{S}_0^{(0)})^2 d\xi},\qquad(73)$$

while in the large-wavelength limit (region A_1 in Fig. 3), the relaxation of the conserved parameter dominates and Ω_{Sc} is given by Eq. (72).

In Fig. 3 we have plotted, for $\tau=0.5$, the inner region dispersion relation given by Eq. (70) as well as the particular limits given by Eqs. (72) and (73) respectively. We have used the experimental value for $\mu_1=0.1P$ [13], and the value of $\Gamma_c=1.5\times10^{-9}$ cm^3 s/g was chosen to have the same velocity unit for the both order parameters $l_S/t_S=l_c/t_c$. There is a transition between these two regimes that takes place when $\Omega_{Sc}(k\rightarrow\infty)=\Omega_c$, which gives

$$k_{c_1}=\frac{(c_{\text{iso}}-c_{\text{nem}})^2}{2\Gamma_c\mu_1\int_{-\infty}^{\infty}(d_\xi\hat{S}_0^{(0)})^2 d\xi},\qquad(74)$$

which for $\tau=0.5$ gives $k_{c_1}=2.8\times10^4$ cm^{-1} with the corresponding critical wavelength $\lambda_{c_1}\simeq 2.2$ μm.

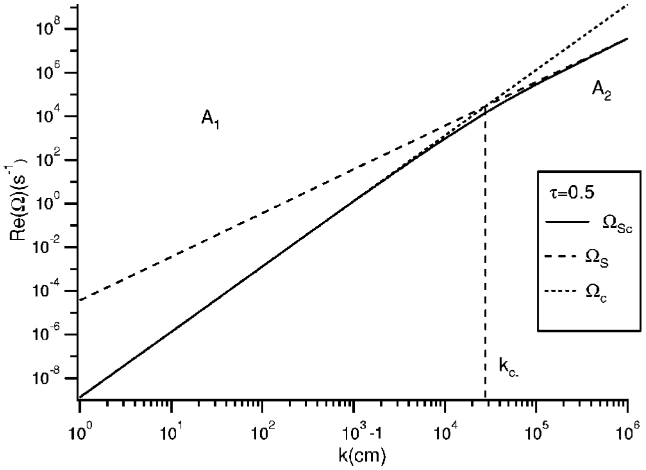

FIG. 3. The inner region (leading-order) damping rate $\text{Re}(\Omega_{Sc})$ (continuous curve) as a function of the wave number k, for $\tau=0.5$, defining two distinct regimes. The nonconserved order parameter dispersion relation Eq. (73) (dashed curve) and conserved parameter dispersion relation Eq. (72) (dotted curve). Region A_1, relaxation of the concentration is the important process; region A_2, relaxation of the orientational order parameter dominates.

In view of the important role played in the dynamics by the quantity k_{c_1}, we attempt here to further interpret this quantity. Equation (74) can be rewritten as

$$k_{c_1}=\frac{1}{2}(c_{\text{iso}}-c_{\text{nem}})^2\frac{1}{\Gamma_c\mu_1}\frac{K_S}{\gamma_S}=\frac{1}{2}(c_{\text{iso}}-c_{\text{nem}})^2\frac{t_c}{t_S}l_S^{-1},\qquad(75)$$

where $t_c=l_S^2/\Gamma_c f_0$ is the relaxation time of the concentration, and $t_S=3\mu_1/2f_0$ is the relaxation time of the orientational order parameter. To deduce these expressions, we have used Eqs. (33) and (34). In writing the first line in Eq. (75), we used also the definition $\gamma_S=K_S\int_{-\infty}^{\infty}(d_\xi\hat{S}_0^{(0)})^2 d\xi$ of the nematic-isotropic interfacial tension for a pure nematogen. The second line of Eq. (75) is written as a ratio times the inverse of the fundamental microscopic length in the problem, as discussed in Sec. III. The ratio involves two quantities, one intrinsic—the ratio of the concentration to orientational relaxation times—and one extrinsic—the square of the concentration difference.

In Fig. 4, we have plotted the phase diagram in the space (τ,k_{c_1}). In region A_1 $(k<k_{c_1})$, the conserved parameter relaxation is the important process, while in region A_2 the nonconserved order parameter relaxation dominates. Near $\tau=1$, the relaxation of the nonconserved order parameter is the important process for all values of k, except a very small region near $k=0$. With decreasing temperature, the concentration variation becomes more and more important, and the

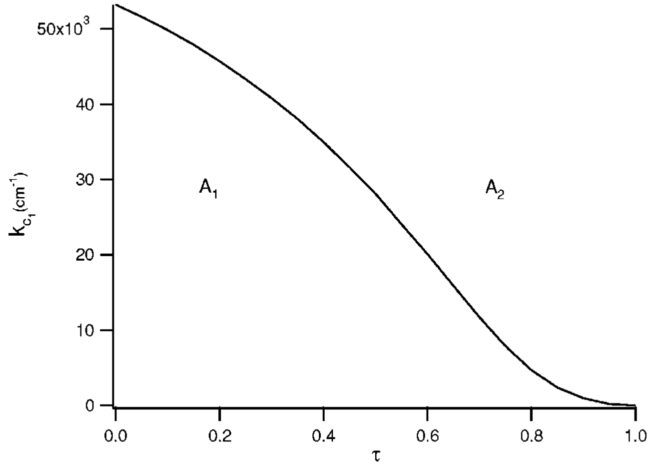

FIG. 4. The phase diagram (τ, k_{c_1}). Region A_1, relaxation of the concentration is the important process; region A_2, relaxation of the orientational order parameter is dominant.

relaxation of the conserved order parameter is dominant in a larger region.

To sum up, we have obtained the leading-order dispersion relation Eq. (52) in the outer regions B and C of dimension l_η. In this region, the interface is sharp and can be considered as a surface of discontinuity. The physics is governed by the dissipation due to shear flow and the dispersion relation is the classical capillary wave dispersion relation at a sharp interface between two fluids with the same densities and different viscosities.

In the inner region A of dimension l_S, without considering the interaction between velocity and the order parameter relaxation, we have obtained the leading-order dispersion relation Eq. (68). In this region, the interface is diffusive and the relaxation of the order parameters is the dominant process.

The important point here is that both the leading-order solutions for the eigenvalues in the inner and outer regions are approximations of the same eigenvalue problem given by Eqs. (36)–(40). Therefore, in the transition region between the inner and outer layers, the two expansions must give the same result. The next step is to combine them into a single expression by matching these two asymptotic expansions.

V. GENERAL DISPERSION RELATION

Now, we consider the interaction between hydrodynamics and relaxation of the order parameters. For details of the method, we refer the reader to our earlier paper [3]. We perturb the base state as follows:

$$\hat{u}^{(0)}(\zeta,\xi,t) = 0 + A\hat{U}(\xi)\exp(ikx - \Omega t),$$

$$\hat{w}^{(0)}(\zeta,\xi,t) = 0 + A\hat{W}(\xi)\exp(ikx - \Omega t),$$

$$p^{(0)}(\zeta,\xi,t) = p_0(\xi) + AP(\xi)\exp(ikx - \Omega t). \tag{76}$$

Substituting these forms and Eqs. (65) into Eqs. (53)–(57), linearizing in A, and eliminating $\hat{U}$ and P, gives

$$(\tilde{\rho}\Omega - \eta k^2)\hat{W} = \left(\frac{\tilde{\rho}\Omega}{k^2} - 3\eta\right)d_\xi^2\hat{W} + \frac{2\eta}{k^2}d_\xi^4\hat{W} - H_1(\mathcal{S},\mathcal{C})d_\xi\hat{S}_0^{(0)} - H_2(\mathcal{S},\mathcal{C})d_\xi\hat{c}_0^{(0)}, \tag{77}$$

$$\mu_1\Omega\mathcal{S} = H_1(\mathcal{S},\mathcal{C}) + \mu_1\hat{W}d_\xi\hat{S}_0^{(0)}, \tag{78}$$

$$\frac{\Omega - \hat{W}d_\xi\hat{c}_0}{\tilde{\Gamma}_c}\int_{-\infty}^{\infty} d\xi' G_k(\xi - \xi')\mathcal{C}(\xi') = H_2(\mathcal{S},\mathcal{C}), \tag{79}$$

where $\eta = \eta_N$ for $\xi < 0$ and $\eta = \eta_I$ for $\xi > 0$ and

$$H_1(\mathcal{S},\mathcal{C}) = -\vec{\nabla}^2\mathcal{S} - K_0\vec{\nabla}^2\mathcal{C} + \frac{\partial^2(\Delta g)}{\partial S^2}(S_0,c_0)\mathcal{S} + \frac{\partial^2(\Delta g)}{\partial c\partial S}(S_0,c_0)\mathcal{C},$$

$$H_2(\mathcal{S},\mathcal{C}) = -K_c\vec{\nabla}^2\mathcal{C} - K_0\vec{\nabla}^2\mathcal{S} + \frac{\partial^2(\Delta g)}{\partial c^2}(S_0,c_0)\mathcal{C} + \frac{\partial^2(\Delta g)}{\partial S\partial c}(S_0,c_0)\mathcal{S}.$$

Integrating Eq. (77) over all ξ, multiplying Eq. (78) by $d_\xi S_0^{(0)}$ and Eq. (79) by $d_\xi c_0^{(0)}$, and integrating, using Eqs. (17) and (68), the following result is obtained:

$$(\tilde{\rho}\Omega - \eta k^2)\int_{-\infty}^{\infty}\hat{W}d\xi + \frac{\Omega}{\Omega_{Sc}}\gamma k^2 = \mu_1\int_{-\infty}^{\infty}\hat{W}(\xi)(d_\xi\hat{S}_0^{(0)})^2 d\xi + \tilde{\Gamma}_c^{-1}\int_{-\infty}^{\infty}d\xi \times\int_{-\infty}^{\infty}d\xi'\hat{W}(\xi)G_k(\xi - \xi')\mathcal{C}(\xi')(d_\xi\hat{c}_0^{(0)})^2. \tag{80}$$

Using the matching condition,

$$\lim_{\xi\to\pm\infty}\hat{W}(\xi) = \frac{1}{\epsilon}\lim_{z\to\pm 0}W^{(0)}(z), \tag{81}$$

Eq. (80) can be rewritten as

$$(\rho\Omega - \eta k^2)\int_{-\infty}^{\infty}W^{(0)}dz + \frac{\Omega}{\Omega_{Sc}}\gamma k^2 = W^{(0)}(0)\left[\mu_1\int_{-\infty}^{\infty}(d_\xi\hat{S}_0^{(0)})^2 d\xi + \Gamma_c^{-1}\int_{-\infty}^{\infty}d\xi \times\int_{-\infty}^{\infty}d\xi' G_k(\xi - \xi')\mathcal{C}(\xi')(d_\xi^{(0)}\hat{c}_0)^2\right]. \tag{82}$$

Using Eqs. (45)–(50), the continuity of horizontal velocity at the interface, and the small-argument limit $1/2k$ of the Green function, we obtain the generalized dispersion relation, in unscaled units,

$$\Omega(\Omega-\Omega_{Sc})=\frac{\mu_1\int_{-\infty}^{\infty}(d_\xi\hat{S}_0^{(0)})^2d\xi+l_S(c_{\mathrm{iso}}-c_{\mathrm{nem}})\int_{-\infty}^{\infty}(d_\xi\hat{c}_0^{(0)})^2d\xi/2k\Gamma_c}{\mu_1\int_{-\infty}^{\infty}(d_\xi\hat{S}_0^{(0)})^2d\xi+(c_{\mathrm{iso}}-c_{\mathrm{nem}})^2/2k\Gamma_c}\Omega_\eta^2, \qquad (83)$$

where Ω_{Sc} is the leading-order dispersion relation in the inner region Eq. (70) and Ω_η is the leading order dispersion relation in the outer region Eq. (52).

The real part of the solution of Eq. (83) and its asymptotic limits given by Eqs. (52) and (70) are drawn in Fig. 5. Three regions can be clearly distinguished. In the short-wavelength limit (region A in Fig. 5), the interface is diffuse and the relaxation of the order parameters is the dominant process. The dispersion relation is given by Eq. (70) (dashed curve in Fig. 5). We note that in region A, the inner region dispersion relation has its asymptotic form given by Eq. (73) (see Fig. 3), meaning that the relaxation of the nonconserved order parameter is dominant.

In the long-wavelength limit, the viscous damping process in the outer region dominates and the corresponding dispersion relation is given by Eq. (52) (dotted curve in Fig. 5). The transition between these two regions takes place when $\mathrm{Re}(\Omega_\eta)=\mathrm{Re}(\Omega_{Sc})$, which gives for $\tau=0.5$ the critical wave number $k_{c_2}\simeq 2.2\times 10^4$ cm^{-1} and the corresponding critical wavelength $\lambda_{c_2}\simeq 2.9$ μm. Two regions can be further distinguished in the hydrodynamics limit. The region B_1 corresponds to $k<k_*\simeq 1$ cm^{-1}, the damping process dominates, and the interface mixture behaves as an interface between two isotropic fluids. Finally, the intermediate region B_2 corresponds to $k_*<k<k_{c_2}$. In this range of the wave numbers, the relaxation of the conserved order parameter plays an important role and cannot be ruled out.

The slope discontinuities of the two curves in Fig. 5 indicate the points where the propagating components cancel $[\mathrm{Im}(\Omega)=0]$, i.e., a transition between a week damping regime where $|\Omega_0|\gg \eta k^2/\rho$ and a strong damping one where $|\Omega_0|\ll \eta k^2/\rho$. The concentration variation induces a decrease of the wave number corresponding to the transition between these two regimes (in the pure nematic system the transition takes place at $k\simeq 10$ cm^{-1}, while in the mixture the transition takes place at $k=k_*$).

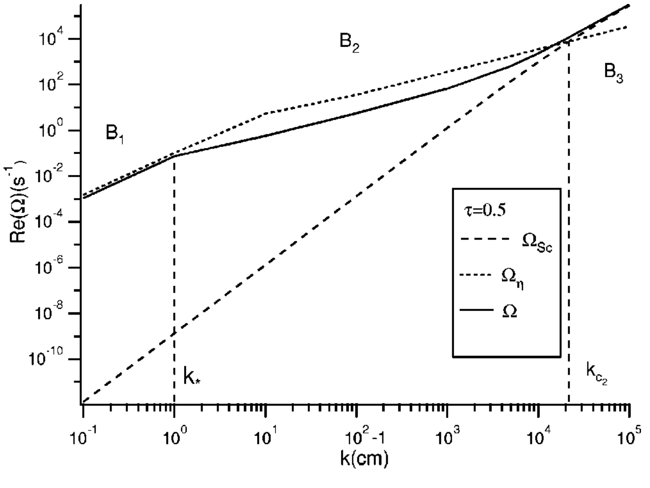

FIG. 5. The damping rate $\mathrm{Re}(\Omega)$ as a function of k for $\tau=0.5$. The general dispersion relation Eq. (83) (continuous curve), the inner region dispersion relation Eq. (70) (dashed line), and the outer region dispersion relation Eq. (52) (dotted curve).

The phase diagram in the space (τ,k_{c_2}) is plotted in Fig. 6. In region B_2 $(k<k_{c_2})$ hydrodynamics is important, while in region A $(k>k_{c_2})$ the relaxation of the nonconserved order parameter and concentration dominate. We note that for a pure nematic system, the transition between regions B_2 and A takes place at $k_{c_2}\simeq 9.5\times 10^3$ cm^{-1}. The second region extends with decreasing temperature and consequently with increasing concentration variation, but the variation is very low.

VI. CONCLUSIONS

In this paper, we have examined surface modes at the nematic-isotropic interface in thermotropic nematic–non-nematic mixtures.

We have used a free-energy density model $f(c,Q_{\alpha\beta})$ as a sum of two terms. The first term is the free-energy density of the isotropic mixing for the two components Eq. (4) of Flory type. The second term is a generalized form of the Landau–de Gennes free-energy density in which we have included the coupling between c and $Q_{\alpha\beta}$ from microscopic considerations Eq. (5). The two representative phase dia-

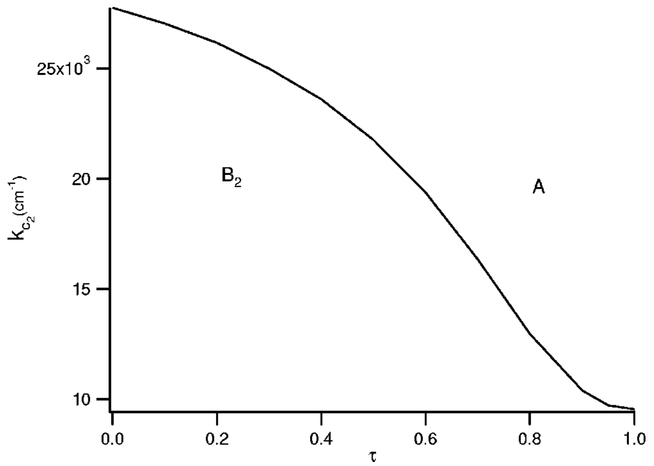

FIG. 6. The (τ,k_{c_2}) phase diagram. Region B_2, hydrodynamics is dominant; region A, the relaxation of the orientational order parameter and concentration govern the physics.

grams generated by this form of the free energy were presented in Fig. 1.

We have considered a planar nematic-isotropic interface in equilibrium. Minimizing the free-energy functional, we have obtained the Euler-Lagrange equation for the equilibrium profiles of the order parameters and the interfacial tension for the two phase diagrams presented. We mention that this interface constitutes the base state in the inner region of the dynamical system.

To explore the dynamics of this system, we have supplemented the Hess-Olmsted-Goldbart-Qian-Sheng model for the orientational, nonconserved, order parameter with the Cahn-Hilliard equation for the conserved parameter, the concentration. We have assumed an isothermal system, characterized by a scalar order parameter S. In this way, we have considered an isotropic interfacial tension, i.e., independent of the director orientation at the interface and neglected all coupling between the director and the hydrodynamic flow. In this model, both phases have the same density, but different viscosities. We have considered the equilibrium planar nematic-isotropic interface as the base state of the system. The front was then perturbed with a small-amplitude monochromatic plane wave and the linear stability of the front was examined.

In the outer region, in the leading order, the key result is Eq. (52). This is the classical dispersion relation for the damping of capillary waves.

In the inner region, ignoring the interaction between the hydrodynamics and the order parameter dynamics, in the leading order, the problem is model C in the Hohenberg and Halperin classification. This couples a nonconserved dynamics governed by the time-dependent Ginzburg-Landau equation and a conserved dynamics described by the Cahn-Hilliard equation. In this approximation, we have obtained the dispersion relation in the inner region Eq. (68), which we have plotted in Fig. 3. Two distinct regions can be distinguished. In the small-wavelength limit, for $k > k_{c_1}$, the relaxation of the nonconserved order parameter is the important process. In the long-wavelength limit, for $k < k_{c_1}$, the relaxation of the conserved parameter becomes dominant. So, ignoring hydrodynamics degrees of freedom, the addition of a conserved parameter has a profound effect on the dynamics at long wavelengths. The critical wave number k_{c_1} which defines the transition between these two regions was obtained [Eqs. (74) and (75)] and plotted in Fig. 4 as a function of temperature.

Using the method of matching asymptotic expansions, we have obtained the generalized dispersion relation Eq. (83). The corresponding relaxation rate is plotted in Fig. 5. Three distinct regions can be distinguished. (i) At very low values of the wave number $k < k_*$, in region B_1, the nematic behaves as an isotropic fluid and the dissipation due to shear flow dominates; (ii) at intermediate values of $k_* < k < k_{c_2}$, in region B_2, the influence of the conserved parameter is important; and finally (iii) at large values of $k > k_{c_2}$, in region A, the relaxation of the nonconserved order parameter governs the physics. In a pure nematogenic system, also three regions must be clearly distinguished (see Fig. 1 in Ref. [4]). In the long-wavelength limit, the dissipation due to shear flow dominates; at intermediate values of wavelength curvature, elasticity and backflow effects play an important role; and finally at small wavelengths the relaxation of the nonconserved order parameter is important. Therefore, even though the two figures look similar, the differences are significant.

We mention that the calculation is simplified as it neglected the coupling between the nematic director and the hydrodynamics flow, as well as the anchoring effect of the director at the interface. We did not use the complete set of Leslie viscosities. Nevertheless, it seems likely that much of the physics will be retained in the general case. However, particularly when the boundary condition at the interface is planar, or when there are anchoring transitions as one goes along the phase coexistence line, there may be interesting new extra physics in the dynamics.

The method we have used will also permit the inclusion of the coupling between interface oscillations, the director field, and the velocity, by including backflow effects. A further complication involves addition of the density. This will allow the study to include interfaces in lyotropic liquid crystals.

ACKNOWLEDGMENTS

V.P.N. and S.K. thank the School of Mathematics, University of Southampton for scientific hospitality. V.P.N. acknowledges support from a Royal Society grant and thanks P. Oswald for fruitful discussions. S.K. thanks COSLAB for funding his visit to Southampton.

---

[1] *Liquid Crystals in Complex Geometries*, edited by G. P. Crawford and S. Zumer (Taylor & Francis, London, 1996).

[2] P. Ziherl, A. Šarlah, and S. Žumer, Phys. Rev. E **58**, 602 (1998); A. Šarlah and S. Žumer, *ibid.* **60**, 1821 (1999).

[3] V. Popa-Nita and T. J. Sluckin, Phys. Rev. E **66**, 041703 (2002).

[4] V. Popa-Nita and P. Oswald, Phys. Rev. E **68**, 061707 (2003).

[5] S. Hess, Z. Naturforsch. A **31a**, 1507 (1976).

[6] P. D. Olmsted and P. Goldbart, Phys. Rev. A **41**, 4578 (1990); **46**, 4966 (1992).

[7] T. Qian and P. Sheng, Phys. Rev. E **58**, 7475 (1998).

[8] J. W. Cahn and J. E. Hilliard, J. Chem. Phys. **28**, 258 (1958); **31**, 688 (1959).

[9] V. Popa-Nita, P. Oswald, and T. J. Sluckin, Proceedings of the ILCC, Ljubljana, 2004 [Mol. Cryst. Liq. Cryst. (to be published)].

[10] P. D. Olmsted and C.-Y. D. Lu, Phys. Rev. E **60**, 4397 (1999).

[11] M. Doi and S. F. Edwards, *The Theory of Polymer Dynamics* (Clarendon, Oxford, 1989).

[12] P. G. de Gennes and J. Prost, *The Physics of Liquid Crystals*,

2nd ed. (Oxford University Press, Oxford, 1993).
[13] P. Oswald and P. Pieranski, *Les Cristaux Liquides: Concepts et Propriétés Physiques Illustrés par des Expériences* (Gordon and Breach Science Publishers, 2000), Vol. 1.
[14] P. J. Flory, *Principles of Polymer Chemistry* (Cornell University Press, Ithaca, 1953).
[15] R. L. Humphries, P. J. James, and G. R. Luckhurst, J. Chem. Soc., Faraday Trans. 2 **68**, 1031 (1972).
[16] J. Katriel, G. F. Kventsel, G. R. Luckhurst, and T. J. Sluckin, Liq. Cryst. **1**, 337 (1986).
[17] P. M. Chaikin and T. C. Lubensky, *Principles of Condensed Matter Physics* (Cambridge University Press, Cambridge, 1995).
[18] A. Matsuyama, R. M. L. Evans, and M. E. Cates, Eur. Phys. J. E **9**, 79 (2002); Z. Lin, H. Zhang, and Y. Yang, Phys. Rev. E **58**, 5867 (1998).
[19] I. Lelidis and G. Durand, J. Phys. II **6**, 1359 (1996).
[20] N. V. Madhusudana and R. Pratibha, Mol. Cryst. Liq. Cryst. **89**, 249 (1982).
[21] S. Faetti and V. Palleschi, J. Chem. Phys. **81**, 6254 (1984); Phys. Rev. A **30**, 3241 (1984); J. Phys. (France) Lett. **45**, L313 (1984).
[22] J. L. Ericksen, Arch. Ration. Mech. Anal. **4**, 231 (1960).
[23] F. M. Leslie, Q. J. Mech. Appl. Math. **19**, 357 (1966); Arch. Ration. Mech. Anal. **28**, 265 (1968).
[24] M. H. Holmes, *Introduction to Perturbation Methods* (Springler-Verlag, Berlin, 1995).
[25] L. D. Landau and E. M. Lifshitz, *Fluid Mechanics* (Pergamon Press, Oxford, 1959).
[26] V. G. Levich, *Physicochemical Hydrodynamics* (Prentice-Hall, Englewood Cliffs, NJ, 1962).
[27] P. C. Hohenberg and B. I. Halperin, Rev. Mod. Phys. **49**, 435 (1977).
[28] A. Shinozaki and Y. Oono, Phys. Rev. E **47**, 804 (1993); A. J. Bray, *ibid.* **58**, 1508 (1998).
[29] J. S. Langer, Ann. Phys. (N.Y.) **41**, 108 (1967); J. Zittartz, Phys. Rev. **154**, 529 (1967); A. J. Bray, Phys. Rev. E **58**, 1508 (1998); W. van Saarloos, Phys. Rep. **301**, 9 (1998).